Title
Optical changes of dentin in the near-IR as a function of mineral content

Authors
Berg, Rhett A
Simon, Jacob C
Fried, Daniel
et al.

Publication Date
2017-02-14

DOI
10.1117/12.2256745

Peer reviewed

HHS Public Access

Author manuscript

Proc SPIE Int Soc Opt Eng. Author manuscript; available in PMC 2017 April 25.

Published in final edited form as:

Proc SPIE Int Soc Opt Eng. 2017 January 28; 10044: . doi:10.1117/12.2256745.

Optical changes of dentin in the near-IR as a function of mineral content

Rhett A Berg, **Jacob C Simon**, **Daniel Fried**, and **Cynthia L Darling**

University of California, San Francisco, San Francisco, CA 94143-0758

Abstract

The optical properties of human dentin can change markedly due to aging, friction from opposing teeth, and acute trauma, resulting in the formation of transparent or sclerotic dentin with increased mineral density. The objective of this study was to determine the optical attenuation coefficient of human dentin tissues with different mineral densities in the near-infrared (NIR) spectral regions from 1300–2200 nm using NIR transillumination and optical coherence tomography (OCT). N=50 dentin samples of varying opacities were obtained by sectioning whole extracted teeth into ~ 150 μm transverse sections at the cemento-enamel junction or the apical root. Transillumination images were acquired with a NIR camera and attenuation measurements were acquired at various NIR wavelengths using a NIR sensitive photodiode. Samples were imaged with transverse microradiography (gold standard) in order to determine the mineral density of each sample.

Keywords

light scattering; dentin; near-IR imaging

1. INTRODUCTION

Only within the last year have new imaging arrays become available to image beyond 1700-nm the limit of conventional InGaAs sensors. Within this newly accessible wavelength range from 1700–2300-nm, light absorption by water is 3–4 times greater and there is a further reduction in light scattering. Recent studies [1–5] suggest that there is reduced scattering at the longer NIR wavelengths for greater optical penetration in bone and soft tissues. The purpose of this study was to determine if there was a similar reduction in optical attenuation in dentin at near-IR wavelengths from 1300–2200-nm.

In addition, we examined root section with varying mineral content to determine how the mineral content influences the optical attenuation in the near-IR. Root fractures may be more visible at longer wavelengths in the NIR. High transparency of sclerotic dentin may enable detection of root fractures using NIR imaging and optical coherence tomography[6, 7].

Several *in vitro* and *in vivo* studies have shown that the near-IR region is highly promising for imaging dental caries due to the high transparency of sound enamel [8–15]. Upon demineralization, the scattering coefficient increases by almost two orders of magnitude which provides high contrast for imaging in both transillumination and reflectance [16]. Optical coherence tomography has also been most successful at 1310-nm for imaging teeth

due to the high transparency of enamel [17–19]. Light scattering in enamel appears to be dominated by Rayleigh scattering and the magnitude of Rayleigh scattering is inversely proportional to the fourth power of the wavelength[20]. Therefore, the magnitude of light scattering in enamel decreases markedly from the UV to the near-IR. Light scattering in dentin is primarily due to the dentinal tubules which behave as cylindrical Mie scatterers. The wavelength dependence is more complex and measurements from 500–1050-nm do not show the marked reduction is scattering that has been observed for enamel [20–23]. Hyperspectral reflectance measurements of Zakian [15] show that the dentin gets darker with increasing wavelength even when water absorption is not increasing. In a study we carried out a few years ago we failed to observe a significant decrease in light scattering from 1300–1650-nm [24].

In order to accurately measure the internally optical properties it is extremely important to reduce the influence of surface scattering. In previous studies of dental enamel, samples were placed in an index matching bath of the same refractive index, namely carbon disulfide or a cargille liquid [8, 20]. In this study the samples were measured in a Cargille liquid to avoid surface scattering.

2. MATERIALS AND METHODS

2.1 Sample Preparation

Fifty previously extracted human canine/premolars with suspected sclerotic dentin deposits were collected and sterilized with gamma radiation. Teeth were visually examined and those determined to contain sclerotic dentin were selected. Teeth were transversely sectioned near the CEJ or apically at the root, using an IsoMet 5000 wet saw from Buehler (Lakebluff, Illinois), of thicknesses ranging from ~100–300 μm. One mesial-distal slice from each tooth was mounted on black orthodontic acrylic rods. Samples were stored in a moist environment of 0.1% thymol to maintain tissue hydration and prevent bacterial growth. The samples underwent transillumination at 1300 nm to determine the areas of transparent dentin. These areas were then examined using long-pass (LP) and band-pass (BP) filters at LP1500, BP1675, BP1920 and BP2200 nm. The areas in question were subjected to histological examination with polarized light microscopy and transverse microradiography.

2.2 NIR Transillumination

Sections underwent transillumination at 1300 nm using a system consisting of a broadband light source Model SLS20 from ThorLabs (Newton, NJ) with LP1500, BP1675, BP1920 and BP2200 filters (Fig. 1). Light beam intensity was modulated using an optical chopper (Stanford Research Systems – SR540 Chopper). Light beams were focused through a custom sample holder consisting of samples fully immersed in a quartz cuvette (1-cm^2) filled with a certified refractive index liquid (n=1.4460 +/− .0002) from Cargille Labs (Cedar Grove, NJ). This procedure ensured that the position of the incident knife-edge beam profiling techniques. collimated light beam was fixed while cycling through all the filters. Phase sensitive detection was employed using a lock-in amplifier (model SR 850) and an optical chopper from Stanford Research Systems (Stanford, CA). The setup for the attenuation measurements is described in Figure 1. Measurements of collimated

transmission were recorded at designated sections of each sample determined to consist of higher content of transparent dentin. The collimated signal (I) at the detector was compared with the initial intensity of the beam (I_o). Using the ratio and the thickness of the samples (d), the attenuation coefficient (μ_t) was calculated using Beer-Lambert plots:

$$\mu_t = -ln(I/I_o)/d.$$

Beer's Law states the intensity of light passing through a sample decreases exponentially as thickness increases. This overall decrease is known as attenuation or extinction, which is caused by diffuse reflection, internal scattering and absorption. The aperture setting was selected to ensure that light scattering at small angles did not significantly contribute to the collimated transmission.

2.3 Polarized Light Microscopy (PLM)

Polarized light microscopy (PLM) was used for histological examination using a Meiji Techno RZT microscope (Saitama, Japan) with an integrated digital camera, Canon EOS Digital Rebel XT (Tokyo, Japan). Sample sections were imbibed in deionized water and examined in the bright field mode with crossed polarizers and a red I plate with 550-nm retardation. Thin sections were subjected to histological examination by polarized light microscopy. Figure 2 shows a thin section of dentin in the visible, NIR and under polarized light.

2.4 Digital Transverse Microradiography (TMR)

A custom-built digital TMR system was used to measure mineral loss in the sample. A high-speed motion control system with UTM150 and 850G stages and an ESP300 controller Newport (Irvine, CA) coupled to a video microscopy and laser targeting system was used for precise positioning of the tooth samples in the field of view of the imaging system. The volume percent mineral for each sample thin section was determined by comparison with a calibration curve of X-ray intensity vs. sample thickness created using sound enamel sections of 86.3±1.9 vol.% mineral varying from 50 to 300-μm in thickness using IgorPRO image analysis software. The calibration curve was validated via comparison with cross-sectional microhardness measurements, $r^2 = 0.99$ [25]. Image line profiles 100–150 pixels in width were extracted from the sample ROI representing the percent mineral at each pixel.

Figure 3 show a mineral density map of one of the dentin sections. Line profiles were drawn through the area of the section at the same location where the intensity was measured in transillumination and the mineral density was taken from a region of interest (ROI) for each tooth section.

3. RESULTS AND DISCUSSION

Figures 4 and 5 show plots of the optical attenuation coefficient for each wavelength calculated from Beer's law versus the volume percent mineral density obtained from transverse microradiography. Figure 4 shows a plot for the mineral density for dentin tooth slices sectioned near the cementum enamel junction while Fig. 5 shows plots sectioned near

the apical root. Unfortunately, we cannot identify any trends with either wavelength or mineral content from these data sets. We had anticipated that the optical attenuation would drop markedly with increased mineral content but that was not apparent from this study. In addition, there was no significant decrease in the optical attenuation with wavelength. The large contribution in attenuation from water absorption and the large surface scattering make these measurements very challenging and we plan to repeat these measurements in the future.

Acknowledgments

This work was supported By NIH/NIDCR Grant R01-DE14698 and the UCSF Summer Research Fellowship program.

References

1. Sordillo LA, Pu Y, Pratavieira S, Budansky Y, Alfano RR. Deep optical imaging of tissue using the second and third near-infrared spectral windows. J Biomed Opt. 2014; 19(5):056004. [PubMed: 24805808]
2. Weber JR, Baribeau F, Grenier P, Emond F, Dubois S, Duchesne F, Girard M, Pope T, Gallant P, Mermut O, Moghadam HG. Towards a bimodal proximity sensor for in situ neurovascular bundle detection during dental implant surgery. Biomed Opt Express. 2013; 5(1):16–30. [PubMed: 24466473]
3. Tachikawa N, Yoshimura R, Ohbayashi K. Cross-sectional imaging of extracted jawbone of a pig by optical coherence tomography. Lasers in Dentistry XVII Proc SPIE. 2011; 7884:F1–7.
4. Sordillo LA, Pu Y, Sordillo PP, Budansky Y, Alfano RR. Deep tissue imaging of microfracture and non-displaced fracture of bone using the second and third near-infrared therapeutic windows. Proc Spie Proc SPIE. 2016; 8926:V1–7.
5. Sordillo DC, Sordillo LA, Sordillo PP, Alfano RR. Fourth Near-Infrared Optical Window for Assessment of Bone and other Tissues. Photonic Therapeutics and Diagnostics XII Proc SPIE. 2016; 9689:J1–7.
6. Shemesh H, van Soest G, Wu MK, van der Sluis LW, Wesselink PR. The ability of optical coherence tomography to characterize the root canal walls. J Endod. 2007; 33(11):1369–73. [PubMed: 17963966]
7. Shemesh H, van Soest G, Wu MK, Wesselink PR. Diagnosis of vertical root fractures with optical coherence tomography. J Endod. 2008; 34(6):739–42. [PubMed: 18498903]
8. Jones RS, Fried D. Attenuation of 1310-nm and 1550-nm Laser Light through Sound Dental Enamel. Lasers in Dentistry VIII Proc SPIE. 2002; 4610:187–190.
9. Bühler CM, Ngaotheppitak P, Fried D. Imaging of occlusal dental caries (decay) with near-IR light at 1310-nm. Optics Express. 2005; 13(2):573–582. [PubMed: 19488387]
10. Fried D, Featherstone JD, Darling CL, Jones RS, Ngaotheppitak P, Buhler CM. Early caries imaging and monitoring with near-infrared light. Dental clinics of North America. 2005; 49(4): 771–93. [PubMed: 16150316]
11. Jones RS, Huynh GD, Jones GC, Fried D. Near-IR Transillumination at 1310-nm for the Imaging of Early Dental Caries. Optics Express. 2003; 11(18):2259–2265. [PubMed: 19466117]
12. Lee C, Lee D, Darling CL, Fried D. Nondestructive assessment of the severity of occlusal caries lesions with near-infrared imaging at 1310 nm. J Biomed Opt. 2010; 15(4):047011: 1–8. [PubMed: 20799842]
13. Staninec M, Lee C, Darling CL, Fried D. In vivo near-IR imaging of approximal dental decay at 1,310 nm. Lasers in Surgery and Medicine. 2010; 42(4):292–8. [PubMed: 20432277]
14. Staninec M, Douglas SM, Darling CL, Chan K, Kang H, Lee RC, Fried D. Nondestructive Clinical Assessment of Occlusal Caries Lesions using Near-IR Imaging Methods. Lasers in Surgery and Medicine. 2011; 43(10):951–959. [PubMed: 22109697]

15. Zakian C, Pretty I, Ellwood R. Near-infrared hyperspectral imaging of teeth for dental caries detection. Journal of Biomedical Optics. 2009; 14(6):064047–7. [PubMed: 20059285]
16. Darling CL, Huynh GD, Fried D. Light scattering properties of natural and artificially demineralized dental enamel at 1310 nm. Journal of Biomedical Optics. 2006; 11(3):34023. [PubMed: 16822072]
17. Colston BW, Sathyam US, DaSilva LB, Everett MJ, Stroeve P. Dental OCT. Optics Express. 1998; 3(3):230–238. [PubMed: 19384365]
18. Feldchtein FI, Gelikonov GV, Gelikonov VM, Iksanov RR, Kuranov RV, Sergeev AM, Gladkova ND, Ourutina MN, Warren JA, Reitze DH. In vivo OCT imaging of hard and soft tissue of the oral cavity. Optics Express. 1998; 3(3):239–251. [PubMed: 19384366]
19. Fried D, Xie J, Shafi S, Featherstone JD, Breunig TM, Le C. Imaging caries lesions and lesion progression with polarization sensitive optical coherence tomography. Journal of Biomedical Optics. 2002; 7(4):618–27. [PubMed: 12421130]
20. Fried D, Featherstone JDB, Glena RE, Seka W. The nature of light scattering in dental enamel and dentin at visible and near-IR wavelengths. Appl Optics. 1995; 34(7):1278–1285.
21. ten Bosch, JJ., Zijp, JR. Optical properties of dentin. IRL Press; Oxford, England: 1987.
22. Zijp JR, ten Bosch JJ. Angular dependence of HeNe laser light scattering by bovine and human dentine. Archs Oral Biol. 1991; 36:283–289.
23. Zijp JR, ten Bosch JJ. Theoretical model for the scattering of light by dentin and comparison with measurements. Appl Optics. 1993; 32:411–415.
24. Chan AC, Darling CL, Chan KH, Fried D. Attenuation of near-IR light through dentin at wavelengths from 1300–1650-nm. Lasers in Dentistry. 2014; 8929:M1–5. XX.
25. Darling CL, Featherstone JDB, Le CQ, Fried D. An automated digital microradiography system for assessing tooth demineralization. Lasers in Dentistry VX. 2009; 7162:1–7.

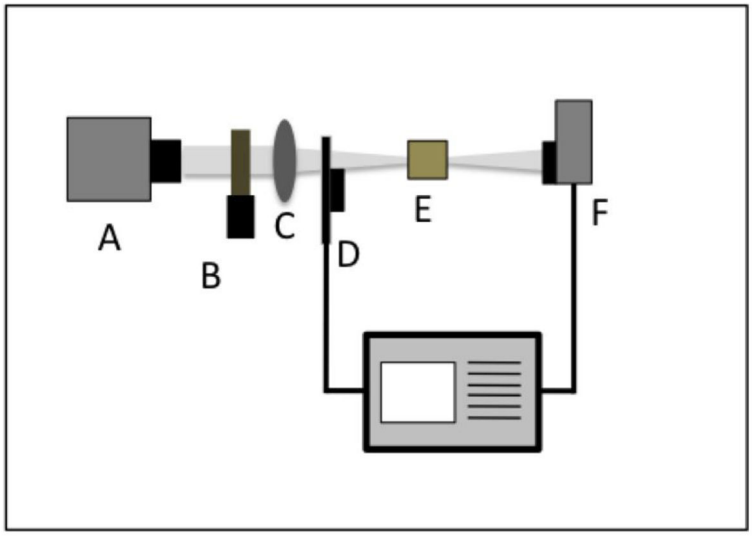

Fig. 1.

The experimental setup for measurement of the optical attenuation through thin sections of dentin placed in a cuvette. (A) Tungsten–halogen lamp with (B) filter wheel, (C) collimating and focusing lenses, optical chopper (D), sample cuvette (E) and (F) detector are shown.

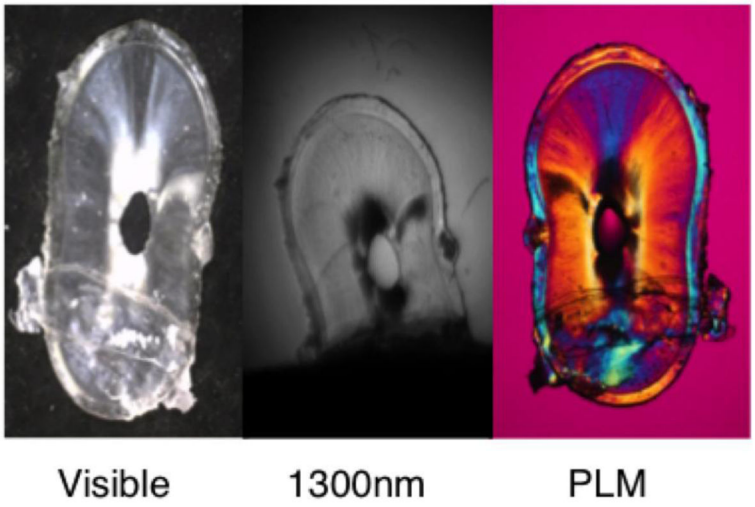

Fig. 2.
Image of a thin tooth section of transparent dentin shown in the visible, the NIR at 1300 nm, and on with polarized light microscopy.

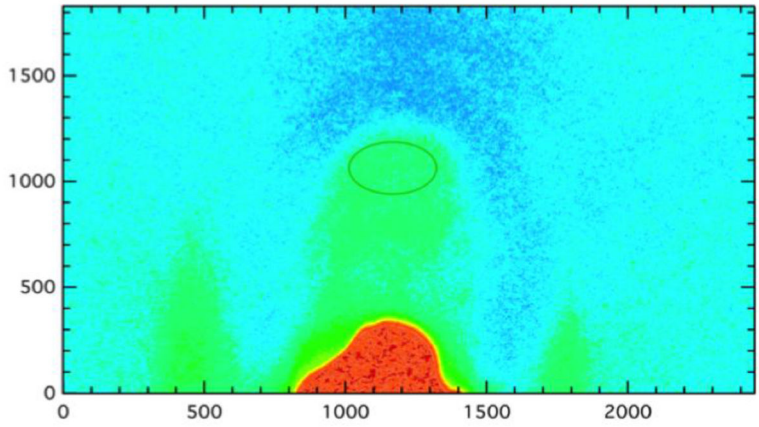

Fig. 3.

Mineral Density map showing the transverse microradiograghy of the transparent dentin sample in Fig. 2. Volume percent mineral measurements were taken at the green oval circle. X and Y axis are in microns.

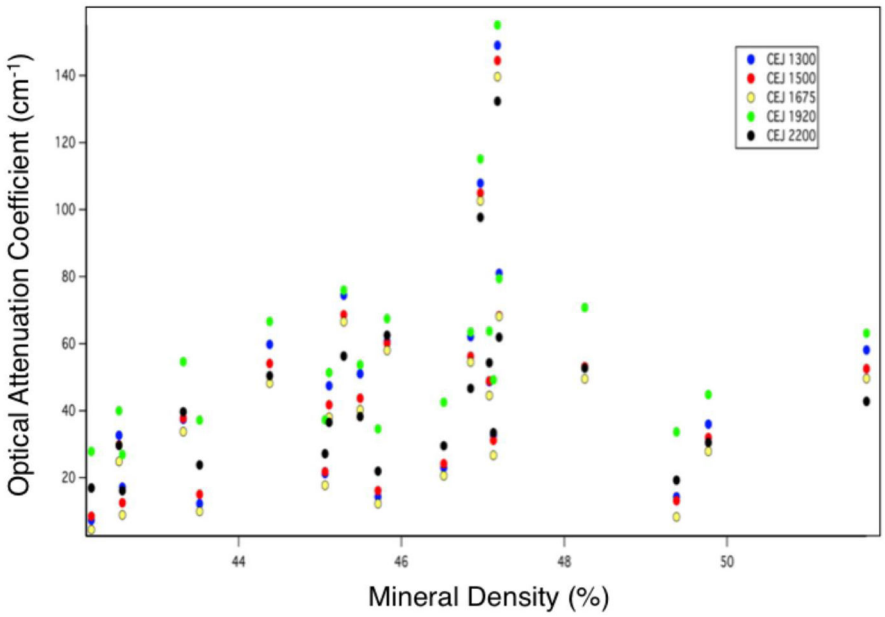

Fig. 4.

The graph shows the optical attenuation coefficient versus the volume percent mineral density for the transparent dentin samples sectioned near the cementum enamel junction.

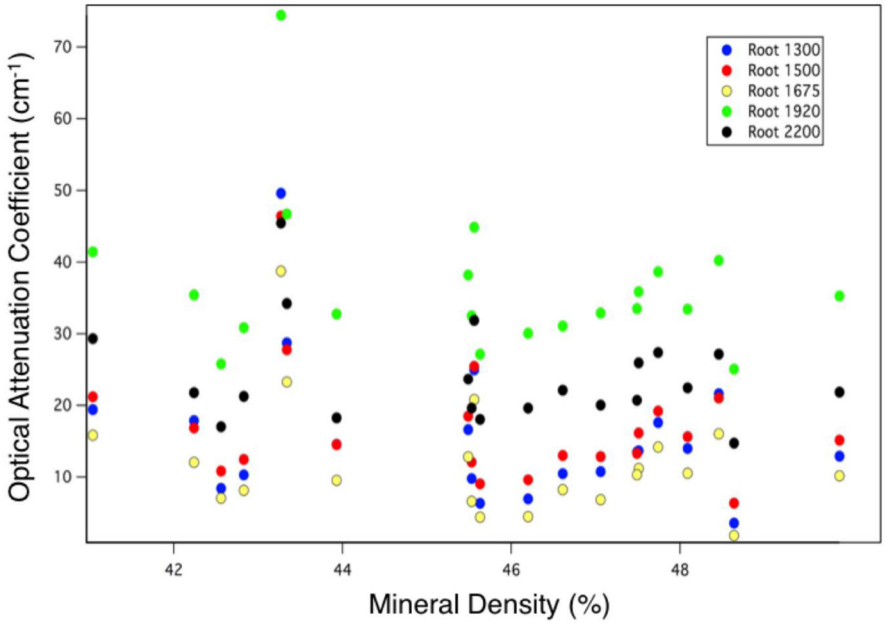

Fig. 5.

The graph shows the optical attenuation coefficient versus the volume percent mineral density for the transparent dentin samples sectioned near the apical root.